A Taguchi-based hybrid multi-criteria decision-making approach for optimization of performance characteristics of diesel engine fuelled with blends of biodiesel-diesel and cerium oxide nano-additive

Sazia Khanam[1] · Osama Khan[1] · Shafi Ahmad[1] · Ahmad F. Sherwani[1] · Zahid A. Khan[1] · Ashok Kumar Yadav[2] · Ümit Ağbulut[3]

Abstract

Given the pressing demand and ongoing necessity for fossil fuels, there is an imperative to actively seek alternative resources to replace petroleum-based fuels. The presents study considers a problem of experimentally investigating the effect of varying levels of important input parameters of a diesel engine fuelled with a novel blend of biodiesel-diesel and cerium oxide nano-additive on the sustainable performance characteristics of a diesel engine. Four input parameters, i.e., blend percentage (B in %), nanoparticle concentration (NPC in ppm), engine load (LD in %) and ignition pressure (IP in bar) each at four levels are considered. Experiments are conducted as per the Taguchi's L_{16} standard orthogonal array and for each experiment, performance parameters (such as Brake thermal efficiency (BTE) and brake specific fuel consumption (BSFC)), emission measures (Carbon monoxide (CO), oxides of nitrogen (NOx), unburnt hydrocarbons (UBHC) and Vibration level (VL)) of the diesel engine are collected. A hybrid multi-criteria decision-making (MCDM) approach, i.e., integrated MEREC-MARCOS method along with signal-to-noise (S/N) ratio and analysis of mean (ANOM) is employed to determine optimal setting of the input parameters that yield optimal multiple performance characteristics. The results reveal that B at 40%, NPC at 80 ppm, LD at 50% and IP at 200 bar is the optimal setting of the input parameters that produce optimum values of the output responses considered simultaneously. Further, results of the analysis of variance (ANOVA) show that Nanoparticle concentration percentage contribution is the maximum (79.63%) followed by engine load (8.40%), ignition pressure (6.28%), and blend percentage (2.11%). The optimization results are: BTE is 32.87%, BSEC is 0.285, CO is 0.018%, NOx is 559.6 ppm, UBHC is 28.1 ppm and VL= 19.57m²/sec which were validated with a confirmation test. Henceforth, such hybrid fuels provide sustainable energy solutions and environmental conservation simultaneously addressing the current and future demands.

Keywords Biodiesel · Biosynthesized nanoparticles · Thermal efficiency · Hybrid optimization · Diesel engine · Acoustic analysis · Renewable energy

✉ Osama Khan
osamakhan6165@gmail.com

✉ Ashok Kumar Yadav
ashokme015@gmail.com

✉ Ümit Ağbulut
umit.agbulut@yildiz.edu.tr

1 Department of Mechanical Engineering, Jamia Millia Islamia (A Central University), New Delhi 110025, India

2 Department of Mechanical Engineering, Raj Kumar Goel Institute of Technology, Ghaziabad 201003, India

3 Department of Mechanical Engineering, Mechanical Engineering Faculty, Yildiz Technical University, 34349, Besiktas, Istanbul, Türkiye

Introduction

Over the last two decades, a sharp increase in conventional energy consumption, notably from crude oil and coal, has led to a rapid depletion of these resources worldwide [1]. This surge is fueled by global industrialization, population growth, and a slow shift toward renewable energy alternatives [2]. The impact of dwindling conventional energy sources is particularly pronounced in underdeveloped and developing countries with larger populations [3]. Additionally, the persistent rise in inflation and oil prices has intensified the ongoing fuel crisis. In the current scenario, many researchers predict a significant surge in crude oil prices, attributed to both escalating inflation and the depletion of

existing oil fields [4]. The current trajectory of fuel prices is expected to continue its upward trend until researchers devise a viable, sustainable, and cost-effective alternative to existing fossil fuels [5]. Declining crude oil reserves, escalating energy dependence, and environmental degradation due to conventional fuel consumption have prompted researchers to explore cleaner, renewable energy resources [6].

A sense of urgency can be felt among the masses to opt for a sustainable and cleaner fuel since the pandemic has emphasized the desire of a healthy ambience with reduced air pollution [7]. Exhaust pollutant particles released from automobiles lead to respiratory diseases. Moreover, these particles amalgamate with other infection carrying microorganisms which can be extremely detrimental to human health, thereby increasing the chances of community spread for viruses such as MERS, SARS and COVID-19. A strong correlation between daily deaths reported due to COVID-19 and growing vehicle pollution levels caused by predominantly small particles ranging between 2.5 and 3 ppm leading to more (2nd and 3rd) lockdowns in several countries has been reported in the literature [8]. Other researchers also reported similar correlation between bad air quality index (AQI) and rising coronavirus cases in states with high population index [9, 10].

Biofuels can be obtained by multiple energy requiring processes such as pyrolysis and transesterification reaction [11, 12]. High initial cost, inferior production quality, improper physiochemical properties, and complex production procedures are the major barriers for universal adoption of the biofuels globally [13, 14]. The major barrier to the global acceptance of secondary oils is the requirement of substantial land for farming which might not be advisable in nations with large scale population [15, 16]. Conversely, third generation of biofuels such as waste cooking oils [17], leachate oils [18], Eichhornia crassipes oil [19] employ waste products to generate engine proficient fuels which proved to be a cost-effective and a sustainable solution[20, 21]. In various studies biodiesel generated from waste cooking oil (WCO) was explored whose physiochemical attributes such as calorific value, density and viscosity were appreciably beneficial to diesel engine performance [22–25]. Landfill solid waste is also explored to derive biofuels in earlier researches [26] Hence, WCO biodiesel can emerge as an economical and viable substitute for sustainable engine operation while contemplating the future predicted depletion of conventional resources. Researchers have explored the potential of combining nano-additives with biodiesel, and they have reported an enhancement in physiochemical characteristics of the biodiesel caused by it [27–34].

Often physical and chemical methods are considered dangerous for environment since production of NPs using these methods also results in emission of poisonous and detrimental substances. Furthermore, these processes require special custom-built equipment, simultaneously consuming substantial amount of power, making the entire process expensive and non-feasible. In particular, the physical procedure for the production of NPs requires additional facilities including surplus aerosol chemical, ultraviolet radiation, and thermal decomposition reactor. As far as chemical conversion techniques are concerned, they too require costly substances as catalyst such as sodium borohydride and reactant stabilizers to stabilize the toxic capacity of the reaction. Conversely, biosynthesized NPs employ plant-based products and reduction takes in a cost friendly and non-toxic mode. These potent plants comprise of polyphenols and proteins which might substitute expensive chemical reactants as transforming agents into metal ions [35–37].

Reaction by-products of biosynthesized NPs can later be utilized for additional purposes in chemical industries. Therefore, this eliminates any harmful by-products released from the reaction which might be difficult to bio-degrade. This not only reduces the power usage but also increases the yield of the final product with lower content of toxic chemicals. For certain plant-based composites, the yield and quality of such biosynthesized NPs are superior to those produced by physical and chemical methods. Thus, it can be inferred that biosynthesized NPs are better in terms of lower emissions rate, enhanced sustainability and better cost-effectiveness.

In the past, researchers have used various MCDM methods in their studies related to the IC engines by methods such as AHP, FAHP, ENTROPY, CRITIC and equal mass were used for computation of the criteria mass and ranking methods viz TOPSIS, VIKOR, WPM, WSM and PROMETHEE, were applied for ranking and selection of the various biodiesel feedstocks [38–43].

Erdoğan et al. (2020) [44] investigated performance, exhaust emissions, and combustion characteristics in a thermal barrier coated (TBC) diesel engine using a multi-criteria decision-making (MCDM) method, specifically operational competitiveness rating (OCRA). The optimal outcome was observed with B20 operating at 1800 rpm. Lamas et al. (2020) [45] investigated the performance and emissions of a marine diesel engine using a numerical model, employing a multiple criteria decision-making (MCDM) approach to identify the optimal injection pattern. To determine criteria masses crucial for MCDM outcomes, the study compared a subjective weighting method with four objective methods: entropy, CRITIC (Criteria Importance Through Intercriteria Correlation), variance, and standard deviation. The incorporation of various nanoparticles induces significant changes in diesel engine performance and emission characteristics, influencing the internal working dynamics of the engine [46, 47]. To comprehend the diverse effects of nanoparticle mixing on diesel engine, a comprehensive literature survey

on various nanoparticles is essential. Soudagar et al. (2021) [48] assessed a modified CRDI diesel engine using Ricinus communis biodiesel with strontium-zinc oxide nanoparticle additives. Results showed an increase in BTE and in cylinder pressure, accompanied by reductions of in BSFC, smoke, Ignition delay, CO, HC, and CO_2. Khan et al. (2020) [49] investigated the application of a blend comprising Nigella sativa biodiesel, diesel, n-butanol, and graphene oxide nanoparticles in a modified CRDI diesel engine. Their findings revealed increased BTE, decreased BSFC, suggesting that a mix with 90 ppm of graphene oxide nanoparticles and 10% n-butanol in Nigella sativa biodiesel is comparable to conventional diesel fuel. Mujtaba et al. (2020) [50] explored a CI engine using a palm–sesame oil blend with oxygenated alcohols and nanoparticles (Carbon Nano Tubes and Titanium oxide). The findings indicated that the B30 and titanium oxide blend exhibited a reduction in BSFC while B30 + DMC showed an increase in BTE. Khan et al. (2023) conducted an experiment using biodiesel-hydrogen and cerium oxide nanoparticles blend and performed MRO of the diesel engine performance parameters, but they used response surface methodology (RSM) rather than MCDM method for optimization [51].

The novelty of current work can be established by stating the fact that to the best of authors knowledge no research has used biosynthesized cerium oxide derived from Ceratonia siliqua in enhancing performance and emission parameters of diesel engine. The uniqueness of the study can also be derived by confirming that optimisation of outputs is achieved by varying nanoparticle concentration and injection pressure which are seldomly chosen together, due to frequent clogging and degradation of inlet valves especially for biofuels with higher viscosity.

While some previous literature discusses the performance of biodiesel and nano-additives in internal combustion engines, there is a notable scarcity of research on optimizing sustainable performance characteristics for diesel engines fueled with biodiesel-diesel blends and biosynthesized nano-additives. This study addresses this gap by experimentally investigating the impact of such blends on diesel engine performance and determining optimal input parameters through the integrated MEREC-MARCOS method. The scarcity of prior work employing this method to enhance engine performance and reduce emissions and vibrations makes this study significant and unique.

Materials and methods

Fuel for diesel engine was prepared by blending biodiesel-diesel and cerium oxide nano-additive. The prepared blends were fuelled in the CI engine, and its sustainable performance characteristics were experimentally investigated. The selection of input parameters and their respective levels is determined by a comprehensive review of prior literature on diesel engines. The study considered feasible experimental ranges that had an apparent impact on outcomes, excluding ranges where no notable changes were observed. Taguchi's design of experiment was used to conduct experiments and for each experiment multiple sustainable performance characteristics of the engine were measured and recorded. A hybrid MCDM method, i.e., integrated MEREC-MARCOS was employed to determine a single index for the considered multiple performance characteristics. Further, Taguchi's approach including S/N ratio, ANOM, and ANOVA was used to determine optimal setting of the input parameters that resulted in the optimum multiple performance characteristics. The results of the study were validated using confirmation test. The detailed aspect of the methodology is described in the subsequent sections. The complete procedure adopted in the present study is shown in the flowchart depicted in Fig. 1.

Preparation of the fuel

Primarily, a fuel was prepared by converting the waste cooking oil (WCO) collected from various local sources such as restaurants and food industries. The available raw oil was then transformed into biodiesel by adding substances such as Methyl alcohol (98.7%), potassium hydroxide (95.8%) and color indicator. In the next step, cerium oxide was obtained from Carob and mixed with biodiesel. Among several previously explored nano-additives, biosynthesized cerium oxide possesses favorable characteristics in bio-energy generation. Its popularity has grown several folds in medical sciences presumably due to its antioxidant and antibacterial capabilities. It is naturally derived from Carob (Ceratonia siliqua) vastly found in Indian subcontinent. Waste leaves of Ceratonia siliqua were obtained from north part of India (Kashmir). The waste leaves were dried in a reactor and grinded to fine particles. Approximately 10 g was weighed and mixed with 100 mL of deionized water. The mixture was placed under an ultrasonic reactor for 20 min. Ultimate mixture was filtered and stored in a cooled area at 2 ℃. A separate salt of Cerium (IV) ammonium nitrate was added in the above prepared mixture in the ratio of 10:100. The solution was again placed under the influence of ultrasonic horn for 10 min at a temperature of 60 ℃. After the mixing, a white paste was formed which was additionally calcined at 200 ℃ for 1 h, resulting in cerium oxide nano-powder.

The produced biodiesel was ultrasonically intermixed with produced biosynthesized Cerium oxide nano-additive (size 30 nm). The mixing process involved weighing the nano-additive and mixing it with distilled water to produce nano-fluid which was subsequently, added to the produced biodiesel. To maintain the stability, surfactant 80 was added
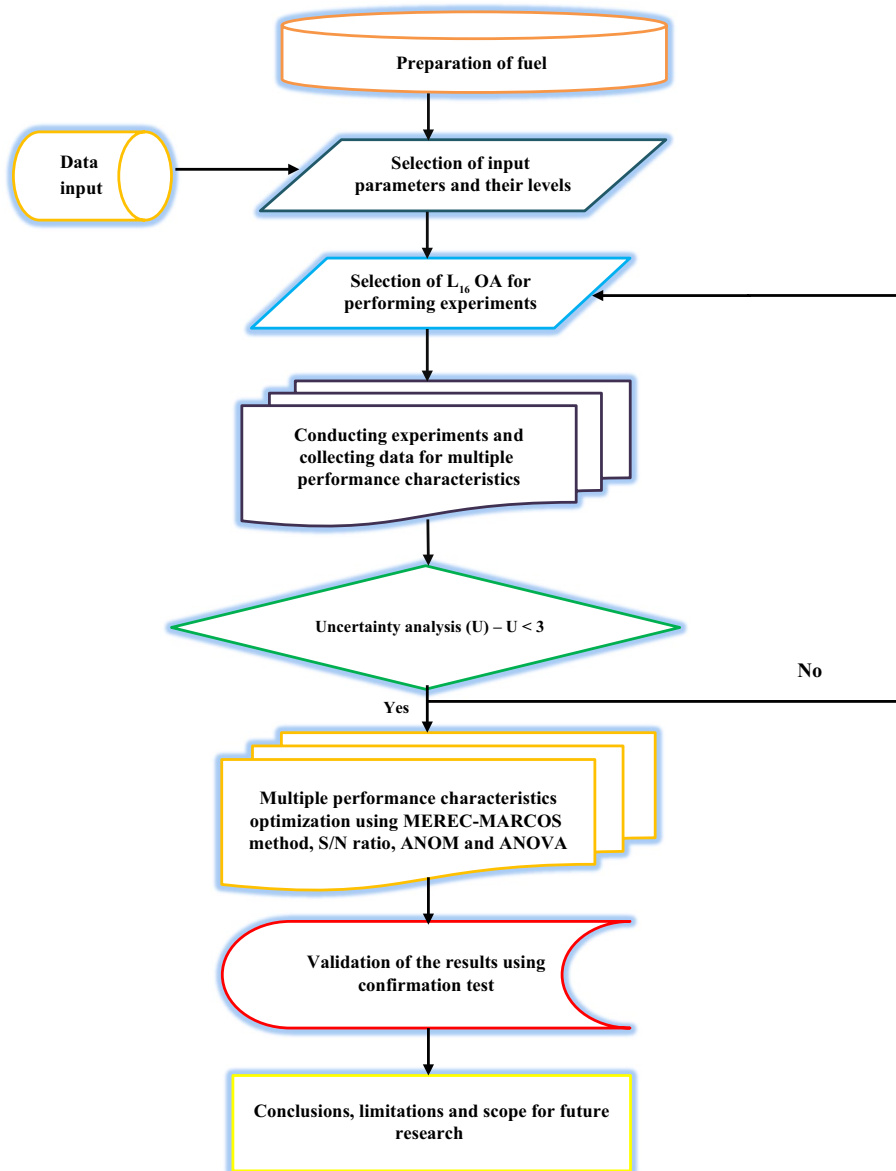
in the biodiesel-cerium oxide mixture which was again inter-mixed by operating the mixture on a magnetic stirrer for prefixed speed of 2500 rpm. Finally, the mixture was placed under an ultrasonic reactor at 110–130 kHz for 25 min. Final composition of the produced fuel contained of 91.8% bio-diesel, 5.1% nano-fluid and 3.1% surfactant on volume basis. Furthermore, blending process was performed in which the obtained hybrid nano-additive biodiesel was blended with pure diesel in different proportions. The fuel obtained was then tested in diesel engine under varying operating con-ditions to estimate the performance, emission and vibra-tion characteristics. The biodiesel-diesel and cerium oxide mixture was tested for various physiochemical properties which were quite alike to petro-diesel fuel as demonstrated in Table 1, thus encouraging its application in CI engine.

Various properties of the final fuel combination of biodiesel-diesel and cerium oxide were compared with the interna-tional ASTM standards as displayed in Table 1.

Selection of the input parameters and their levels

Selection of input parameters plays a vital role in experimen-tal investigation of their effect on the output responses. In the contemporary research four input parameters, i.e., Blend percentage (B), nanoparticle concentration (NPC), engine load (LD) and ignition pressure (IP) were selected based on the past literature whose experimental results have con-firmed their feasibility. It may be noted that B refers to bio-diesel blend percentage where biodiesel-diesel are mixed to form a single fuel in different concentration. NPC specifies

Table 1 Comparison of the physiochemical attributes of the experimental fuels [51]

Properties	Waste cooking oil /WCO	Biodiesel-diesel and cerium oxide	Diesel	ASTM limit
FFA/%	–	1.3	0.0015	Max. 2
Density at 15 °C/kg m^{-3}	884	899	843	860–900
Calorific value /MJ kg^{-1}	49.8	41.93	44.85	Min. 33
Flash point/°C	71.36	105	51	Min. 130
Cetane number/°C	59	55	51.3	Min. 45
Kinematic viscosity /centi-Stoke	3.50	2.8	4.56	2.52–7.5

nanoparticle concentration where nano-additives are powdered into fine particle and mixed with fluids to form nano-fluids. LD represents load applied on the diesel engine where the force acts against the power produced by the engine. IP defines ignition pressure which is the force that makes the top of the piston bulge by applying a gas pressure on the piston. In order to select discrete levels of the input parameters, their feasible range that strongly influenced the output responses was considered. The considered feasible range of B, NPC, LD and IP was 10–40%, 20–80 ppm, 25–100% and 190–220 bars, respectively, and four levels of each input parameter from these ranges were selected. The input parameters and their levels are shown in Table 2. B was not considered beyond 40% since it results in high viscosity and low density, thereby requiring a slight variation in original engine design making the whole process infeasible and expensive. NPC beyond 80 ppm was not considered since some modifications are required in valve timing diagram of the engine, to avoid excessive deposition and increased aggregation of nano-additives concentration, resulting in segregation among sample fuel blends [48]. LD below 25% presents small negligible variations in engine performance and exhaust analysis, hence not considered. IP above 220 bar was not considered as it increases the engine temperature to an abnormal state resulting in engine seize or malfunction.

The concurrent exploration of Nano Particle Concentration (NPC) and Ignition Pressure in diesel engine experimentation involving biodiesel and nanoparticles is seldom preferred due to inherent challenges related to clogging and degradation. The integration of biodiesel and nanoparticles in the experimental setup introduces complexities that can impede the overall performance of the diesel engine. Clogging issues are a common challenge, particularly in the fuel injection system, where nanoparticles may aggregate and

obstruct the flow, leading to reduced efficiency and potential damage. Furthermore, the degradation of nanoparticles over time poses a significant hurdle, impacting their effectiveness and altering the ignition pressure characteristics. In optimizing the fuel injection system, several key considerations are crucial. The injectors are redesigned to enhance the dispersion of nanoparticles within biodiesel, necessitating alterations in the injector nozzle geometry to generate a finer spray pattern and ensure the uniform distribution of the biodiesel-nanoparticle mixture during injection. This also ensures material compatibility serving as a resistant to potential corrosive effects from biodiesel and nanoparticles, thereby prolonging the lifespan of injectors and preventing premature wear. The implementation of variable injection parameters is vital, enabling adjustments based on the specific characteristics of the biodiesel-nanoparticle blend. Controlling and monitoring nanoparticle size within the fuel injection system is imperative to ensure that nanoparticles remain within an optimal size range for combustion, minimizing the risk of clogging.

Taguchi method

Genichi Taguchi developed this statistical method to enhance quality of the manufactured goods. This method postulates that all manufacturing processes get affected by outside factors called noise and it is difficult to identify all the possible sources of noise. However, a few most influential noise factors having significant impact on the product variability can be identified and their effect can be reduced with the help of proper experimental design. This method has been extensively used in engineering design [52], and various researchers have applied it successfully to solve single and multi-response optimization problems [53–56]. There are

Table 2 Input parameters and their levels

Input parameter	Symbol	Unit	Level 1	Level 2	Level 3	Level 4
Blend percentage	B	%	10	20	30	40
Nanoparticle concentration	NPC	ppm	20	40	60	80
Engine load	LD	%	25	50	75	100
Ignition pressure	IP	bar	190	200	210	220

three components, i.e., system design, parameter design, and tolerance design of this method. Among these, the parameter design is the most commonly used procedure [57] which aims at determining the parameters' setting that results in the best quality characteristic/performance measure with minimum variation. To determine the optimal setting of the considered parameters, this method uses a strategically designed experiment with different combinations of the levels of the design/process parameters. Taguchi specified larger-the-better; smaller-the-better; and nominal-the-better, as the quality characteristic of choice. Further, *S/N* ratio is used as the loss function instead of standard deviation in this method because as the mean decreases, the standard deviation also deceases and vice versa. The *S/N* ratio for larger-the-better and smaller-the-better performance characteristics is computed using Eq. (1) and Eq. (2), respectively.

$$S/N = -10\log_{10}\left[\frac{1}{n}\sum_{k=1}^{n}\frac{1}{y_{ijk}^2}\right] \quad (1)$$

$$S/N = -10\log_{10}\left[\frac{1}{n}\sum_{k=1}^{n}y_{ijk}^2\right] \quad (2)$$

where y_{ijk} represents experimentally collected value of the ith performance characteristic in the jth experiment at the kth test and n signifies the number of tests.

In the present study, four levels four input parameters have been considered and therefore, Taguchi's L_{16} orthogonal array (OA) in coded form, as shown in Table 3, was used to conduct experiments to collect experimental results for the multiple performance characteristics.

Table 3 L_{16} OA

Exp. no.	B	NPC	LD	IP
1	1	1	1	1
2	1	2	2	2
3	1	3	3	3
4	1	4	4	4
5	2	1	2	3
6	2	2	1	4
7	2	3	4	1
8	2	4	3	2
9	3	1	3	4
10	3	2	4	3
11	3	3	1	2
12	3	4	2	1
13	4	1	4	2
14	4	2	3	1
15	4	3	2	4
16	4	4	1	3

Experimental setup used for investigation

After preparing multiple blends of biodiesel-diesel and cerium oxide nano-additive, the prepared mixture was fueled in diesel engine where its performance, emission and vibration parameters were experimentally measured according to the L_{16} OA shown in Table 3. The experimental setup is displayed in Fig. 2 which comprised of a single rail direct injection diesel stationary engine. Speed changes were accomplished by varying load applied on the engine directly coupled with an eddy current dynamometer for torque variations. The resistive type of load panel comprised of a voltmeter and current meter. Torque variations for the engine ranged between 0 and 18 kgf. An interactive display was included within the system which demonstrated various other measurements such as fuel tank volume, air flow rate, and fuel consumption. The engine exhausts primarily included unburned hydrocarbon (UBHC), carbon monoxide (CO), and nitrogen oxide (NOx) emissions which were displayed on the screen of gas analyzers. While vibration level was recorded with the help of triaxial accelerometer Piezo-electronics. Table 4 shows the various technical details of the engine setup. The calculation of outcomes is shown in Appendix A.1

Method based on removal effects of criteria (MEREC)

The importance of the various performance characteristics determined in terms of mass plays an important role in the decision-making process. Over the years, several objective methods such as Entropy, Standard Deviation (SD), Mean mass have been developed for computation of the mass of criteria/performance characteristics. MEREC method for determination of criteria masses was proposed by Keshavarz-Ghorabaee et al., [59] which suggests that higher mass to a performance characteristic should be assigned if its removal results in higher change in the aggregate performance of the experiments. This is new a method as compared to others objective mass calculation methods and is relatively less explored, due to which it has been used in this study to determine the masses of the output responses. The steps of this method are discussed as follows [59]:

Step 1: Formulate decision matrix (A) of size $m \times n$ as given by Eq. (3).

$$A = \begin{bmatrix} a_{11} & \cdots & a_{1q} \\ \vdots & \vdots & \vdots \\ a_{p1} & \cdots & a_{pq} \end{bmatrix}_{m \times n} \quad (3)$$
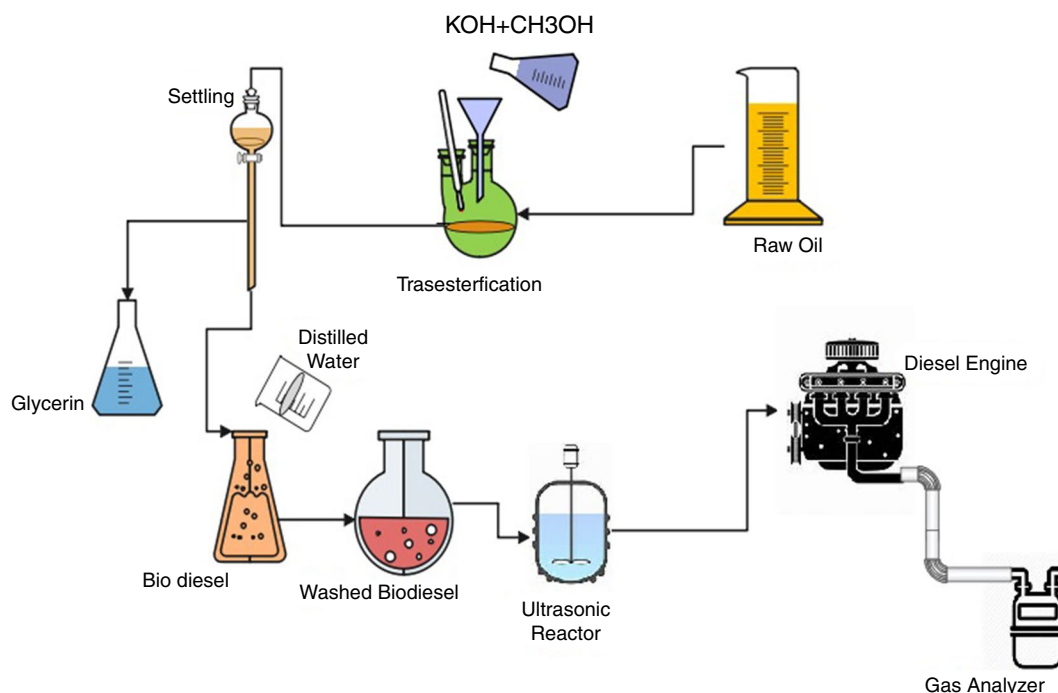
Fig. 2 Graphic representation of the experimental setup

where the value of the performance characteristic q in experiment p is represented by a_{pq}. The variables p and q vary from 1 to m and 1 to n, respectively.

Step 2: Elements of the decision matrix are normalized to transform them into a comparable range using Eq. (4).

$$b_{pq} = \begin{cases} \dfrac{\min_{p}(a_{pq})}{a_{pq}} & q \in beneficial \\[2mm] \dfrac{a_{pq}}{\max_{p}(a_{pq})} & q \in non-beneficial \end{cases} \qquad (4)$$

where the normalized value of the element a_{pq} of A is represented by b_{pq}.

Table 4 Technical specifications of CI engine

S.No	Element	Specification
1	Engine brand	PETTER-AV1
2	Engine category	CRDI, 4-stroke, DI, water-cooled
3	Bore	80 mm
4	Stroke	110 mm
5	Rated power	15 BHP at 1500 rpm
6	Compression ratio	19:1
7	Dynamometer	Eddy current
8	Load sensor	Load cell, type strain gauge
9	Compression pressure	48.15 kg cm^{-2}

Step 3: An overall performance of the alternatives (R_p) which is logarithm measure of the normalized value is computed using Eq. (5).

$$R_p = \ln\left(1 + \left(\frac{1}{m}\sum_{q}\left|\ln\left(b_{pq}\right)\right|\right)\right) \qquad (5)$$

Step 4: The performance of the experiments on removal of a specific performance characteristic (S_{pq}) is computed by eliminating a particular performance characteristic as given by Eq. (6).

$$S_{pq} = \ln\left(1 + \left(\frac{1}{m}\sum_{q,q\neq k}\left|\ln\left(b_{pq}\right)\right|\right)\right) \qquad (6)$$

where k varies from 1 to n.

Step 5: Determine the overall absolute deviations (T_p) of the experiments by subtracting S_{pq} from R_p as given by Eq. (7).

$$T_q = \sum_{p}\left|R_p - S_{pq}\right| \qquad (7)$$

Step 6: Compute mass of the performance characteristics (w_q) by normalizing the values of the T_p as given by Eq. (8).

$$w_q = \frac{T_q}{\sum_q T_q} \tag{8}$$

Measurement alternatives and ranking according to compromise solution (MARCOS) method

MARCOS is a MCDM method used to rank different experiments on the basis of utility degree. This method holds an advantage of maintaining stability of results in the presence of large number of alternatives and criteria [60]. Since its development it has been employed by various researchers to solve decision-making problem such as supplier selection in healthcare industry [61], human resource evaluation in transport industry [62], project management software selection [63] and risk analysis for road traffic [64]. The steps of this method are as follows:

Step 1: Formulate decision matrix (A) by arranging the values of the performance characteristics for each experiment in rows and columns as given by Eq. (3).

Step 2: The formulated decision matrix is extended by inserting anti-ideal (AS) and ideal solution (IS) at the top and bottom, respectively, resulting in the development of extended decision matrix (C) as given by Eq. (9).

$$C = \begin{bmatrix} a_{g1} & \cdots & a_{gq} \\ a_{11} & \cdots & a_{1q} \\ \vdots & \cdots & \vdots \\ a_{p1} & \cdots & a_{pq} \\ a_{h1} & \cdots & a_{hq} \end{bmatrix}_{(m+2)\times n} \tag{9}$$

where $[a_{g1}, a_{g2}, \ldots, a_{gq}]$, $[a_{h1}, a_{h2}, \ldots, a_{hq}]$ represents the AS and IS, respectively, the elements of which are determined using Eqns. (10) and (11), respectively.

$$a_{gq} = \begin{cases} \min_{1 \le p \le m} (a_{pq}) & q \in \text{beneficial} \\ \max_{1 \le p \le m} (a_{pq}) & q \in \text{non-beneficial} \end{cases} \tag{10}$$

$$a_{hq} = \begin{cases} \max_{1 \le p \le m} (a_{pq}) & q \in \text{beneficial} \\ \min_{1 \le p \le m} (a_{pq}) & q \in \text{non-beneficial} \end{cases} \tag{11}$$

Step 3: The elements of *C* are normalized to transform them into similar range using Eq. (12).

$$c_{pq} = \begin{cases} \frac{a_{pq}}{a_{hq}} & q \in \text{beneficial} \\ \frac{a_{hq}}{a_{pq}} & q \in \text{non-beneficial} \end{cases} \tag{12}$$

Step 4: The weighted normalized values (d_{pq}) are computed by multiplying the normalized values with the masses to include the importance of the output responses as given by Eq. (13).

$$d_{pq} = c_{pq} \times w_q \tag{13}$$

where w_q is the mass of the performance characteristic q determined using MEREC method in this study.

Step 5: The utility degree of the experiments in relation to AS and IS represented by E^+ and E^-, respectively, is determined using Eq. (14) and (15), respectively.

$$E_p^+ = \frac{\sum_{q=1}^{n} d_{pq}}{\sum_{q=1}^{n} d_{hq}} \tag{14}$$

$$E_p^- = \frac{\sum_{q=1}^{n} d_{pq}}{\sum_{q=1}^{n} d_{gq}} \tag{15}$$

Step 6: The utility function $f(E)$ representing a compromise of the experiments in relation to AS and IS is computed using Eq. (16).

$$f(E_p) = \frac{E_p^+ + E_p^-}{1 + \frac{1-f(E_p^+)}{f(E_p^+)} + \frac{1-f(E_p^-)}{f(E_p^-)}} \tag{16}$$

where $f(E_p^+) = \frac{E_p^+}{E_p^+ + E_p^-}$ and $f(E_p^-) = \frac{E_p^-}{E_p^+ + E_p^-}$.

Step 7: The utility function is a final value representing a combined performance score of the experiments for multiple performance characteristics. A higher value of $f(E_p)$ suggests that the experimental values are best within the considered set of experiments and the experiment should be ranked first. Further, rank of other experiments decreases with decreasing value of utility function.

The selection of MEREC-MARCOS method for multicriteria decision-making in optimizing the performance parameters of a diesel engine stem from its efficacy in handling complex decision scenarios inherent in this domain. The MEREC-MARCOS method integrates multiple criteria, such as fuel efficiency and emissions, providing a comprehensive framework to evaluate and prioritize competing alternatives. Its ability to accommodate diverse and often conflicting objectives aligns well with the intricate nature of optimizing diesel engine performance. This method employs mathematical modeling and analysis to systematically assess the trade-offs among different criteria, facilitating informed decision-making that balances the need for enhanced efficiency, reduced environmental impact, and economic feasibility.

The selection of the MEREC-MARCOS method for diesel engine analysis is justified by its unique strengths in

Table 5 Overall absolute deviation (T_q) and masses of the performance characteristics

	BTE	BSEC	CO	NOx	UBHC	VL
T_q	0.3865	0.3729	0.3236	0.3000	1.3389	0.3753
W	0.1248	0.1204	0.1045	0.0969	0.4323	0.1212

addressing the intricacies of multi-criteria decision-making specific to this domain. Unlike other methods such as VIKOR, Entropy, and Genetic Algorithms (GA), MEREC-MARCOS excels in handling the complex interplay of criteria crucial for diesel engine optimization. Its emphasis on incorporating environmental, economic, and performance factors aligns well with the diverse and often conflicting objectives inherent in diesel engine design. MEREC-MARCOS's mathematical modeling and analytical rigor make it particularly suitable for evaluating trade-offs between fuel efficiency, emissions reduction, and cost-effectiveness. Its ability to provide a comprehensive understanding of the decision space, considering uncertainties and preferences, sets it apart. In essence, the MEREC-MARCOS method stands out as a robust and tailored approach for diesel engine analysis, offering a nuanced perspective that accounts for the multifaceted challenges in achieving optimal performance.

	BTE	BSEC	CO	NOx	UBHC	VL
T_q	0.3865	0.3729	0.3236	0.3000	1.3389	0.3753
W	0.1248	0.1204	0.1045	0.0969	0.4323	0.1212

Results and discussion

Results

Experiments were performed according to L_{16} OA shown in Table 3 and for each experiment the multiple performance characteristics were measured as per the procedure described in Sect. "Method based on removal effects of criteria (MEREC)". The experimental results are shown in Table 8 as shown Appendix B.

Level	B	NPC	LD	IP
Level 1	− 3.5405	− 4.0513	− 3.6406	− 3.5420
Level 2	− 3.6137	− 3.6387	− 3.3400	− 3.4232
Level 3	− 3.5421	− 3.3756	− 3.5774	− 3.4867
Level 4	− 3.4498	− 3.0804	− 3.5881	− 3.6941
Difference (Max.–Min)	0.0732	0.6758	0.3005	0.1188
Rank	4	1	2	3

The multiple performance characteristics were transformed into a single performance score using MEREC and MARCOS methods. MEREC method was used to

determine the mass of each performance characteristic signifying its importance. The masses so obtained were used in the MARCOS method to compute a single performance score for the six performance characteristics.

The values of the performance characteristics acted as decision matrix for both MEREC and MARCOS methods and for clarity as shown in Table 9 in Appendix.

Source of variation	Degrees of freedom	Sum of square (SS)	Mean square (MS)	% Contribution
B	3	0.0541	0.0180	2.11
NPC	3	2.0375	0.6792	79.63
LD	3	0.2151	0.0717	8.40
IP	3	0.1608	0.0536	6.28
Residual error	3	0.0914	0.0305	3.58
Total	15	2.5588		

Since the units of the performance characteristics were different, they were normalized using Eq. (4) to transform them into a comparable range. It should be noted that BTE is a beneficial performance characteristic as its maximum value is desired and the other five performance characteristics are of non-beneficial type since their minimum values are required. Further, overall performance score and performance score on removal of a specific performance characteristic were computed using Eq. (5) and Eq. (6), respectively. Based on the removal effects of the performance characteristics, overall absolute deviation (T_q) of the experiments was determined using Eq. (7). Subsequently, masses of the performance characteristics were computed using Eq. (8). The overall absolute deviation (T_q) and masses of the performance characteristics so obtained are shown in Table 5.

It can be seen from Table 5 that mass of UBHC is the highest, i.e., 0.4323, and for NOx, it is the lowest, i.e., 0.0969. It suggests that among the considered performance characteristics, UBHC is the most important while NOx is the least important one, respectively. Further, the importance of all the performance characteristics in descending order is UBHC > BTE > Vibration > BSEC > CO > NOx.

Further, MARCOS method was employed to compute utility function representing a single performance score for the six performance characteristics. The decision matrix was extended by inserting the AS and IS at top and bottom using Eq. (9), Eq. (10) and Eq. (11), respectively. The extended

Table 6 ANOM table for *S/N* ratio

Level	B	NPC	LD	IP
Level 1	− 3.5405	− 4.0513	− 3.6406	− 3.5420
Level 2	− 3.6137	− 3.6387	− 3.3400	− 3.4232
Level 3	− 3.5421	− 3.3756	− 3.5774	− 3.4867
Level 4	− 3.4498	− 3.0804	− 3.5881	− 3.6941
Difference (Max.–Min)	0.0732	0.6758	0.3005	0.1188
Rank	4	1	2	3

decision matrix so obtained was normalized using Eq. (12). Subsequently, the masses obtained using MEREC method were multiplied with the normalized values to determine weighted normalized values using Eq. (13). Based on the weighted normalized value, utility degree in relation to AS and IS was computed using Eq. (14) and Eq. (15), respectively. Finally, the utility function of the experiments was determined using Eq. (16). Since a higher value of the utility function represents the best experiment, a higher-the-better characteristics for $f(E)$ were considered and its signal-to-noise (*S/N*) ratio was computed using Eq. (2). The $f(E)$ value and the corresponding *S/N* ratio so obtained are shown in Table 10 in Appendix.

Table 10 reveals that $f(E)$ value of experiment number 16 is the maximum (0.7146), and therefore, it can be concluded that input parameter setting of this experiment, i.e., B at 40%, NPC at 80 ppm, LD at 25% and IP at 210 bar is the best one for all six performance characteristics taken simultaneously.

It may be noted that a full factorial design that involves four input parameters, each at four levels, has a total of 256 experiments each having a unique combination of the input parameters. However, in the present study, only 16 experiments have been performed as per the Taguchi's L_{16} OA and therefore, it might be possible that the optimal setting of input parameters may not be present in 16 experiments.

Therefore, to obtain optimum setting of the input parameters, Analysis of Mean (ANOM) was performed as suggested by Taguchi. In ANOM, mean value of the *S/N* ratio at each level of the input parameter was computed. For example, the mean value at level 1, level 2, level 3 and level 4 of the input parameter B was obtained by taking arithmetic mean of the *S/N* ratio of Exp. No. 1 to 4, Exp. No. 5 to 8, Exp. No. 9 to 12 an Exp. No. 13 to 16, respectively. Similarly, the mean values of the *S/N* ratio at other levels of the input parameters were computed. The ANOM table for *S/N* ratio is shown in Table 6, and the *S/N* graph is shown in Fig. 3.

Regardless of the performance characteristic whether it is beneficial or non-beneficial, the maximum value of the mean *S/N* ratio is considered to obtain the optimal setting of the input parameters. It can be observed from Table 6 that maximum value of mean *S/N* ratio is obtained at level 4 of B, level 4 of NPC, level 2 of LD and level 2 of IP. Also, the same can be observed from Fig. 3. Hence, it can be concluded that within the investigated range B at 40%, NPC at 80 ppm, LD at 50% and IP at 200 bars is optimal setting of the input parameters that simultaneously optimizes all six performance characteristics considered in the present study. Further, Table 6 also reveals that rank of NPC is 1 which signifies that all six performance characteristics are highly sensitive to a change in NPC. The input parameters in descending order of sensitivity are NPC > LD > IP > B.

Further, to examine the significance of the input parameters for the performance characteristics, analysis of variance (ANOVA) was performed. ANOVA is a standard statistical tool which is used to identify the systematic and random factors of a dataset based on the variability, and the procedure for ANOVA can be found in any standard text of statistics. Results of ANOVA are presented in Table 7.

Table 7 shows that NPC is the most significant input parameter for affecting all performance characteristics as its percentage contribution is the maximum (79.63%), and it is followed by LD (8.40%), IP (6.28%), and B (2.11%).
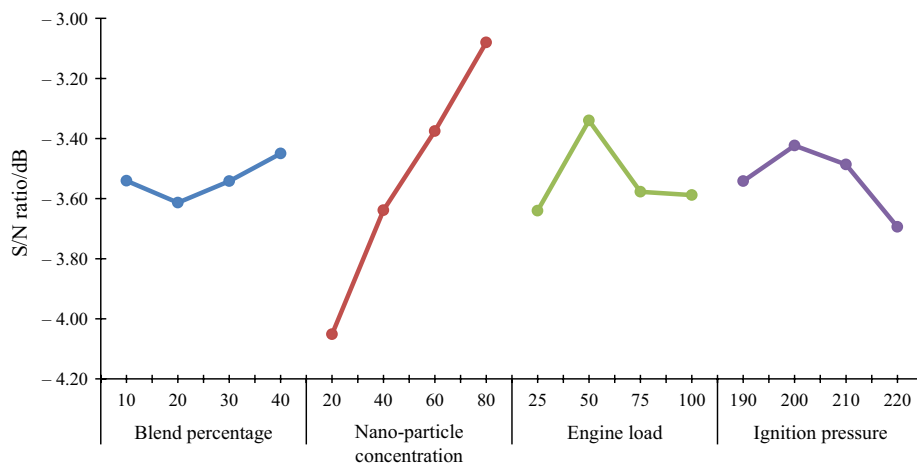
Fig. 3 The *S/N* graph for utility function

Table 7 ANOVA table for *S/N* ratio

Source of variation	Degrees of freedom	Sum of square (SS)	Mean square (MS)	% Contribution
B	3	0.0541	0.0180	2.11
NPC	3	2.0375	0.6792	79.63
LD	3	0.2151	0.0717	8.40
IP	3	0.1608	0.0536	6.28
Residual error	3	0.0914	0.0305	3.58
Total	15	2.5588		

Validation test

The final step was to conduct the confirmation test to validate the results of the study. In the confirmation test, an experiment is conducted at the optimal setting of the input parameters and the performance characteristics of this experiment are measured and recorded. Subsequently, the *f(E)* value, and its corresponding value of *S/N* ratio is computed. Further, predicted value of the *S/N* ratio at the optimal setting of the input parameters is computed using the Taguchi's approach. Finally, the experimental value of the *S/N* ratio is compared with that of the predicted value of the *S/N* ratio and if the two values are found to be in close agreement, then, the result is validated. In the present study, since it was not possible to determine the value of *f(E)* and its corresponding *S/N* ratio for a single experiment run at the optimal setting of the input parameters and therefore, to obtain the experimental value of the *S/N* ratio, a linear regression model between the performance characteristics and the corresponding *S/N* ratio was developed which is given in Eq. (17). The value of the coefficient of determination (R^2) for this linear regression model was found to be very (99.25%) which signifies a very strong relationship between the *S/N* ratio and the performance characteristics.

$$S/N = 4.7611 - 0.0434 \times BTE - 1.5014 \times BSEC$$
$$- 41.865 \times CO - 0.0013 \times NOx - 0.1128 \qquad (17)$$
$$\times UBHC - 0.0534 \times VL$$

An experiment at the optimal combination of the input parameters, i.e., B 40%, NPC 80 ppm, LD 50% and IP 200 bar was performed for which the following performance characteristics were measured: BTE = 32.87%, BSEC = 0.285, CO = 0.018%, NOx = 559.6 ppm, UBHC = 28.1 ppm and VL = 19.57 m^2 sec^{-1}. Substituting these values in Eq. (17) resulted in an experimental value of *S/N* ratio as − 2.782 dB.

The predicted value of the *S/N* ratio, i.e., $(S/N)_{opt}$ at the optimal setting of the input parameters was determined using Eq. (18).

$$(S/N)_{opt} = (S/N)_{mean} + \sum_{i=1}^{n} \left[(S/N)_i - (S/N)_{mean} \right] \qquad (18)$$

where $(S/N)_{mean}$ is the mean value of the *S/N* ratio for all the experiments, $(S/N)_i$ is the mean value of the *S/N* ratio at the optimal level of the input parameter; *i* and *n* is the total number of input parameters.

The predicted value of the *S/N* ratio computed using Eq. (18) was found to be − 2.684 dB. Since the experimental and predicted values are in close agreement (percentage error = 3.65%), the results obtained in the study are validated.
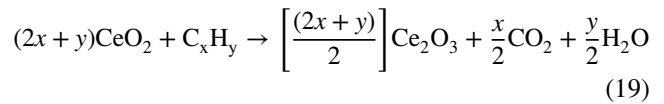
Discussion

The level of importance, determined on the basis of the mass, considered performance characteristics of the diesel engine fuelled with blend of biodiesel-diesel and cerium oxide in decreasing order is found as **UBHC > BTE > Vibration > BSEC > CO > NOx**. Further, the present study suggests that the optimum multiple performance characteristics of the diesel engine are achieved at 40% blend percentage (level 4), 80 ppm nanoparticle concentration (level 4), 50% load application (level 2), and 200 bar injection pressure (level 2).

Prior engine studies have extensively advocated for higher blend percentage between 35 -40% for fuels amalgamated with nanoparticles as lower calorific value and higher viscosity are nullified by superior atomization characteristics due to presence of nanoparticles in fuel, leading to superior BTE and lower BSEC [62, 63]. Superior atomization in turn is achieved by superior heat conduction rate of cerium oxide, which results in quicker evaporation of the test blends. Furthermore, higher concentration of biodiesel facilitates surplus oxygen available for combustion reaction, which in turn is further increased by higher oxidation capacity of the cerium oxide nanoparticle resulting in a wholesome burning process. Subsequently, this leads to lower exhaust emissions like NOx, CO and UBHC as depicted in Fig. 4. While analyzing vibrating components of the engine, pistons reciprocating motion were

considered to be the prime most factor followed by a bunch of other parameters too. Other parameters comprised of combustion pressure, valve timing, engine lubrication requirement, incoming and outgoing fluids which also influenced engine vibrations [67]. Hybrid nano-additive combinations of fuel blends facilitate superior combustion characteristics simultaneously lowering the vibration levels, thereby improving the service life and operational reliability of the engine. Conversely, lower concentration of biodiesel leads to an advanced ignition of fuels is higher quantity of diesel is present in fuel, causing a nonlinear increase in root mean square (RMS) of vibration response which is in close vicinity to the combustion getting developed at TDC [68].

The contemporary research established an optimum value of 80 ppm nanoparticle concentration which is the highest possible level achieved for feasible engine characteristics as shown in Fig. 5. This is also validated by previous literatures since higher NPC facilitates higher surface area eventually enhancing fuel distribution within the

combustion chamber and increasing the BTE value [69, 70]. Successful atomization is achieved with higher NPC which enables the blended oil molecules to get separated into micro molecules, resulting in homogenous dispersal and enhanced infiltration further decreasing BSEC value. Higher NPC value facilitates fuel blends with comprehensive thermal conductance and higher oxygen content leading to an improved mixing reaction for a wholesome combustion process with lower emission values such as UBHC and CO as evident from the Eq. (18) and Eq. (19).

$$(2x + y)CeO_2 + C_xH_y \rightarrow \left[\frac{(2x + y)}{2}\right]Ce_2O_3 + \frac{x}{2}CO_2 + \frac{y}{2}H_2O$$
(19)

$$4CeO_2 + C_{soot} \rightarrow 2Ce_2O_3 + CO_2$$
(20)

Furthermore, the uniform intermixing of nanoparticles with biodiesel results in extended burning period during combustion continuing in diffusion phase, leading to additional energy generation and lowered NOx values as shown in Eq. (20).
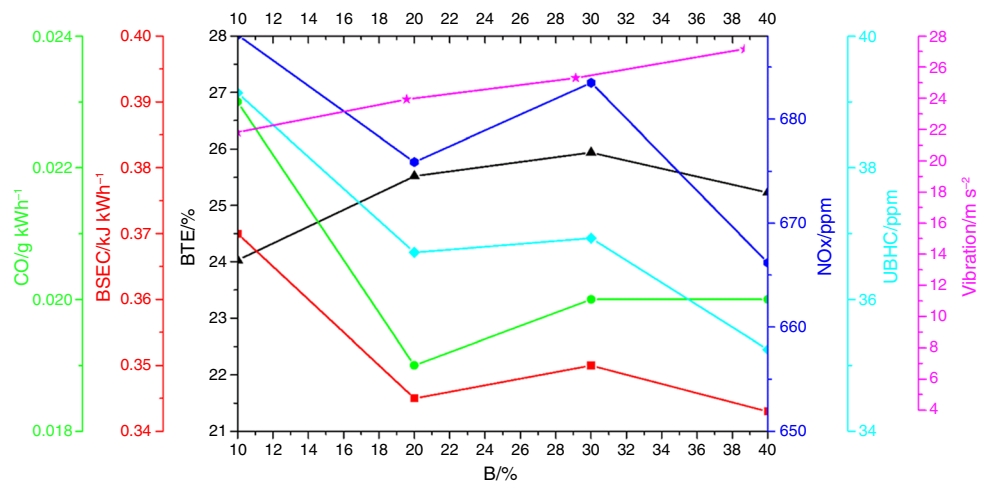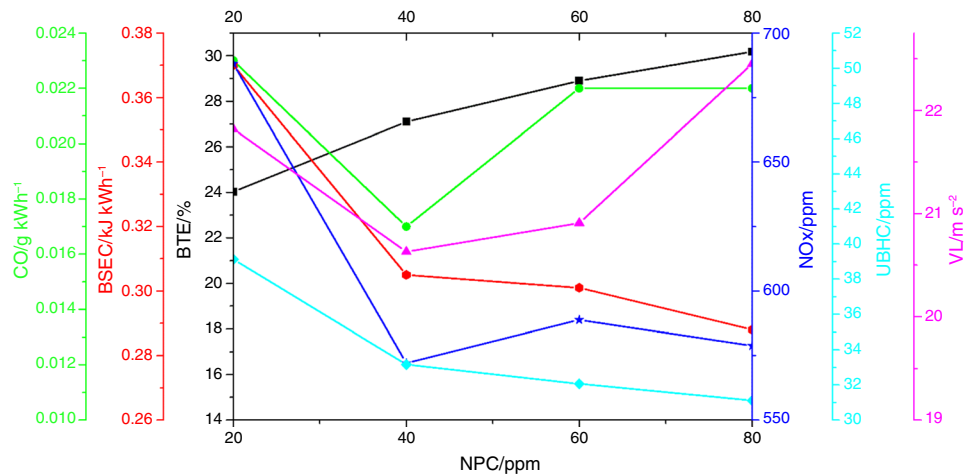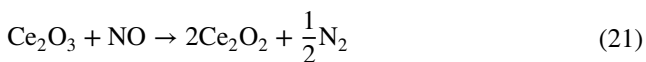

Fig. 4 Impact of blend percentage on outcomes

Fig. 5 Impact of nanoparticle concentration on outcomes

$$Ce_2O_3 + NO \rightarrow 2Ce_2O_2 + \frac{1}{2}N_2 \qquad (21)$$

Significant reductions in vibration levels are achieved at higher NPC range which is quite evident since larger surface area facilitates an ideal combustion process. Also, during abnormal combustion, sudden high-pressure shock waves are released which are extremely detrimental to the engine operation [71].

45–50% is the optimum engine load range obtained for ideal engine outcomes established during experimentation as shown in Fig. 6. Another trend revealed increased BTE value for a lower level of load applied on engine. This is quite evident as higher load application on diesel engine results an imbalance in air fuel ratio. This is due to higher fuel requirement by the engine to perform the requisite action, thereby resulting in abnormal combustion in engine cylinder [72]. Pre-mixed and dispersion combustion stages are the prime parameters which influence BSEC value while varying load application on engine. Therefore, lower levels of load are preferred since it consumes lesser amount of fuel resulting in lower value of BSEC, while at higher loads, the engine has to draw in more fuel for the same power input. A lower delay time, during the pre-mixed stage throughout the diffusion stage, results in a homogeneous fuel mixture. Optimum load application leads to increased atomization, which results in an improved A/F ratio. Consequently, a homogenous fuel–air mixture is achieved, resulting in a shortened latency just before the combustion commences further leading to lower UBHC and CO content [73]. Generally higher cylinder temperature yields higher NOx content in diesel engine. The study also detected lower NOx content analyzed in gas analyser at lower loads which is predominantly due to lower volumes of fuel being pumped inside the chamber. This further translates into lower pressure and temperature being developed in the combustion chamber, considered to be the prime reason for NOx generation [74]. On the contrary, for increased load application on the engine, more volume of fuel is pumped to achieve desired power, thus simultaneously increasing the pressure and temperature constraints of the gases forming within the cylinder which in turn raised NOx content. At higher engine load, the vibration tends to increase since it increases the inertia forces, simultaneously increasing the crank rpm also [75]. Thus, lower levels of load are preferred for lower vibration and superior comfort to the rider and car accessories.

During the experimentation, performance characteristics were explored for various combinations and levels of injection pressure (IP) and the optimum value which achieved ideal engine outcomes was found to be 200 bars as shown in Fig. 7. At this value, a reduction in ignition delay was achieved by speeding up the vaporization of the diesel blend, thereby enabling oil autoignition a bit sooner than previous conditions resulting in superior BTE value. On the other hand, higher IP value results in faster and abnormal fuel burning process, thereby lowering power yield of diesel engine [76]. Bigger oil particles are broken down into finer particles when the injection pressure of the fuel pump is increased, thereby enhancing overall blend atomization. This injection pressure in turn depends on IP value which if optimally controlled can yield better BSEC value. Lower levels of IP value contribute significantly in diminishing the UBHC and CO concentration in exhaust gases. During the initial phase of fuel, the lower IP contributes to the efficient transport and distribution of heat among air and fuel within combustion chamber, leading to a wholesome combustion with minimum UBHC and CO exhaust levels [29]. They also contribute significantly to the reduction in NOx throughout the ignition phase. Prior studies have reported that biofuels deliver higher NOx percentage than conventional diesel oil, and this is indeed a big hurdle in their globalization [77]. Superior atomization for biodiesel-diesel blends is reported, when operated at higher IP, consequently raising the temperature of cylinder. Piston cylinder temperature and oxygen content present within the fuel are the prime factors in estimating the outlet NOx content. Considerably high IP values

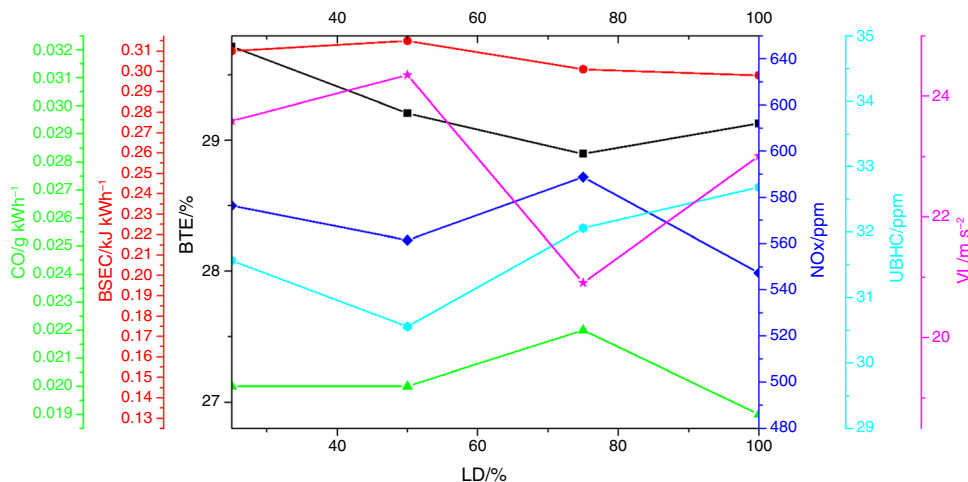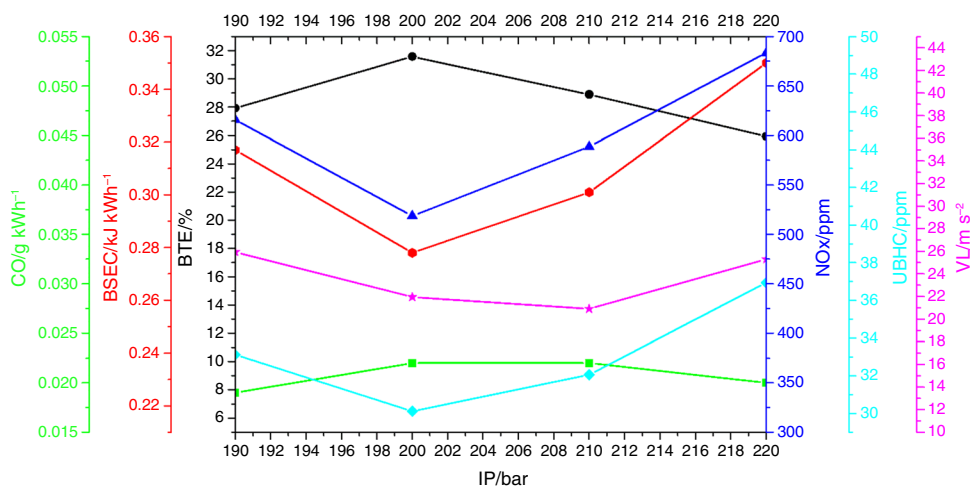**Fig. 6** Impact of load percentage on outcomes

Fig. 7 Impact of ignition pressure on outcomes

increase mean gas temperature, thereby producing higher NOx. Therefore, lower NOx emission levels are achieved at lower IP value. The pressure increments during combustion impact the air–fuel mixture thereby varying the engine vibration signal in an abrupt manner [78]. IP variation is supposedly responsible for increasing rate of oscillation and in cylinder pressure. A high IP value produces complex and high vibration responses due to uneven distribution of temperature and pressure of the gas in the chamber during the combustion process. Hence, lower IP values are preferred for lower vibration levels which is also validated by previous researches[79]. Consequently, the outcomes generated from the MCDM integrated technique is in agreement with the possible technical consequences given by several investigators [47–49].

The adoption of biodiesel-diesel blends with cerium oxide nano-additives is susceptible to external factors, such as policy changes and market trends, which play a pivotal role in shaping the broader context of this study. Policy changes, particularly those related to environmental regulations and incentives for sustainable energy sources, can significantly influence the acceptance and integration of biodiesel blends with nanoparticles in the market. Supportive policies may foster a conducive environment for the adoption of such innovative fuel technologies by providing financial incentives or regulatory frameworks that encourage their use. Conversely, policy shifts that are less favorable to biofuels or nanoparticles may pose challenges and hinder widespread acceptance. Moreover, market trends, including shifts in consumer preferences, industry demands, or advancements in competing technologies, can also impact the feasibility and commercial viability of biodiesel-nano-additive blends. Understanding and analyzing these external factors are crucial for anticipating potential challenges and opportunities, providing a comprehensive context for the study and its implications in the dynamic landscape of energy and transportation.

Conclusions

The new generation in substantial numbers is pondering and contemplating on the impact of conventional energies and thereby crave to make a transition in sustainable energy forms. This transition is probably due to masses opting for a cleaner, cheaper and easily available source of energy. This recent surge in popularity for renewable sources is exploited by researchers to furnish cost-effective and efficient solutions of power generation. Present study explored the potential of waste cooking oil by converting it into biodiesel and later blending the produced biodiesel with novel biosynthesized cerium oxide nano-additive to enhance diesel engine performance and emission measures. Further, it also investigated the sustainable performance characteristics of the diesel engine fueled with the prepared blend. Four input parameters, i.e., B, NPC, LD and IP each at four levels were considered. Diesel engine's performance characteristics such as BTE, BSEC, CO, NOx, UBHC and vibration level were experimentally investigated using Taguchi's L_{16} OA. Multi-performance characteristics optimization was carried out using hybrid MCDM approach, i.e., integrated MEREC-MARCOS method, S/N ratio, and ANOM. Statistical significance of the input parameters for the output responses was established through ANOVA. Finally, multi-performance characteristics optimization result of the study was validated using confirmation test. Results of the present study lead to the following conclusions:

- Biosynthesized cerium oxide nano-additive can be successfully used as an alternative fuel for achieving sustainable performance characteristics of the diesel engine.
- Nanoparticle concentration is the most important one followed by engine load, ignition pressure and blend percentage.

- Blend percentage at 40%, nanoparticle concentration at 80 ppm, engine load at 50% and ignition pressure at 200 bars is the optimal setting.
- Nanoparticle concentration percentage contribution is the maximum (79.63%) followed by engine load (8.40%), ignition pressure (6.28%), and blend percentage (2.11%).
- In the validation test, predicted *S/N* ratio value is − 2.684 dB with a percentage error of 3.65%, indicating a close agreement between experimental and predicted values.

In future, to enhance the comprehensiveness of research on biodiesel and nano-additives, a broader dataset can be obtained by experimenting with various metallic and non-metallic nano-additives blended in biodiesel. Additionally, exploring biodiesel production from alternative sources like eucalyptus, Karanja, seaweed, mustard, soybean would introduce novel blend combinations for diesel engine use. To achieve a more thorough analysis, researchers may consider incorporating a larger number of input parameters with multiple levels. Furthermore, the scope of performance characteristics can be expanded to include additional acoustic parameters such as noise and pressure rise. The application of a full factorial design of experiments could contribute to a systematic and comprehensive experimental investigation. Lastly, a comparative analysis of the performance characteristics across different types of diesel engines (high, medium, and low power) may provide valuable insights into the varied applications of biodiesel blends.

Appendix A

Outcome calculation

In this research, performance characteristics of diesel engine were measured by employing measuring apparatuses, chemical formulas and empirical relations depending upon the type of performance. In the present study, six sustainable performance characteristics were considered and their measurement method is described as follows:

Brake thermal efficiency (BTE) It can be defined as the ratio of the brake power (BP) obtained at the crankshaft to fuel energy (*E*) available to engine for combustion process, and it was computed using Eq. (1).

$$\eta = \frac{BP}{E} \tag{22}$$

where η is the brake thermal efficiency (in %); *BP* is the Brake power (in kW), and *E* is the fuel energy (in kW).

Brake specific energy consumption (BSEC) It is a suggestive parameter which represents the efficiency attained by the engine from specific volume of fuel to produce a single unit power. In mathematical terms, BSEC is the product of applied fuels calorific value (CV) and brake specific fuel consumption (BSFC) and is used to prepare a comparison among various fuels. The specific energy consumption is a more accurate estimate in comparison with specific fuel consumption. It was computed using Eq. (2)

$$BSEC = CV \times BSFC \tag{23}$$

where CV is the calorific value (in kJ kg^{-1}) and BSFC is the brake specific fuel consumption (in kg kWh^{-1}).

Vibration level (VL) The engine vibration level was recorded using Triaxial accelerometer Piezo-electronics. A sensor was attached to the engine which measured acceleration developed in any of the 3-orthogonal axes.

Equation (3) was used for computing total vibration acceleration a_{total} of the engine

$$a_{\text{total}} = \sqrt{a_{\text{vertical}}^2 + a_{\text{lateral}}^2 + a_{\text{longitudinal}}^2} \tag{24}$$

where a_{vertical} is the acceleration in vertical axis (in m sec^{-2}); a_{lateral} is the acceleration in lateral axis (in m sec^{-2}), and $a_{\text{longitudinal}}$ is the acceleration in longitudinal axis (in m sec^{-2}).

CO, NOx, UBHC Lack of the requisite amount of oxygen which accelerates the combustion process is primarily identified as main reason for the development of unburned hydrocarbons (UBHC), carbon oxide (CO) and oxides of nitrogen (NOx). The AVL DIGAS 444N exhaust gas analyzer was employed to measure the volumes of CO emissions in terms of percentage (%) and UBHC and NOx emissions as ppm. The emission levels of CO, UBHC and NOx were converted into ppm and further converted into g kW^{-1} h^{-1} as per the standard exhaust testing method. An example displaying the required conversion system has been shown for carbon monoxide emissions. Emission volumes of CO are generated in terms of ppm which is a standard measuring unit for diesel engine whose formula is given in Eq. (4)

$$CO(g\,kWh^{-1}) = \frac{CO(ppm) \times 1e^{-6} \times \dot{m}_{exh}(gh^{-1}) \times MW_{CO}(gmol^{-1})}{BP(kW) \times MW_{exh}(g\,mol^{-1})} \tag{25}$$

where BP is the brake power; $\dot{m}_{exh}$ is the mass flow rate of exhaust gases; MW_{CO} is the molecular weight of carbon monoxide, and MW_{exh} is the molecular weight of the combined exhaust gases.

Appendix B

See Table 8–10, .

Table 8 Experimental results

Exp. no.	Input parameters				Performance characteristics					
	B /%	NPC/ppm	LD/%	IP (bar)	BTE/%	BSEC/ kJ kWh^{-1}	CO/g kWh^{-1}	NOx (ppm)	UBHC (ppm)	VL/m s^{-2}
1	10	20	25	190	24.030	0.370	0.023	688.102	39.136	21.820
2	10	40	50	200	27.103	0.305	0.017	572.098	33.159	20.630
3	10	60	75	210	28.898	0.301	0.022	588.811	32.059	20.910
4	10	80	100	220	30.186	0.288	0.022	578.773	31.119	22.450
5	20	20	50	210	25.527	0.345	0.019	675.889	36.715	23.940
6	20	40	25	220	28.991	0.334	0.022	650.113	35.312	22.260
7	20	60	100	190	29.131	0.298	0.019	547.331	32.683	23.010
8	20	80	75	200	31.586	0.278	0.022	518.773	30.119	21.950
9	30	20	75	220	25.940	0.350	0.020	683.501	36.931	25.310
10	30	40	100	210	28.157	0.312	0.019	659.909	33.032	26.060
11	30	60	25	200	29.718	0.310	0.020	576.460	31.565	23.590
12	30	80	50	190	32.977	0.282	0.019	546.527	28.902	21.460
13	40	20	100	200	25.230	0.343	0.020	666.201	35.241	27.170
14	40	40	75	190	27.937	0.317	0.019	615.655	33.126	25.940
15	40	60	50	220	29.208	0.315	0.020	561.460	30.555	24.350
16	40	80	25	210	32.573	0.295	0.019	549.527	29.102	20.010

Table 9 Decision matrix

Exp. no.	BTE	BSEC	CO	NOx	UBHC	VL
1	24.030	0.370	0.023	688.102	39.136	21.820
2	27.103	0.305	0.017	572.098	33.159	20.630
3	28.898	0.301	0.022	588.811	32.059	20.910
4	30.186	0.288	0.022	578.773	31.119	22.450
5	25.527	0.345	0.019	675.889	36.715	23.940
6	28.991	0.334	0.022	650.113	35.312	22.260
7	29.131	0.298	0.019	547.331	32.683	23.010
8	31.586	0.278	0.022	518.773	30.119	21.950
9	25.940	0.350	0.020	683.501	36.931	25.310
10	28.157	0.312	0.019	659.909	33.032	26.060
11	29.718	0.310	0.020	576.460	31.565	23.590
12	32.977	0.282	0.019	546.527	28.902	21.460
13	25.230	0.343	0.020	666.201	35.241	27.170
14	27.937	0.317	0.019	615.655	33.126	25.940
15	29.208	0.315	0.020	561.460	30.555	24.350
16	32.573	0.295	0.019	549.527	29.102	20.010

Table 10 $f(E)$ values and the corresponding S/N ratio

Exp. no.	B	NPC	LD	IP	$f(E)$	S/N ratio (dB)
1	10	20	25	190	0.6159	− 4.2101
2	10	40	50	200	0.6916	− 3.2032
3	10	60	75	210	0.6762	− 3.3982
4	10	80	100	220	0.6800	− 3.3504
5	20	20	50	210	0.6354	− 3.9390
6	20	40	25	220	0.6306	− 4.0052
7	20	60	100	190	0.6776	− 3.3802
8	20	80	75	200	0.6974	− 3.1304
9	30	20	75	220	0.6219	− 4.1257
10	30	40	100	210	0.6538	− 3.6913
11	30	60	25	200	0.6739	− 3.4287
12	30	80	50	190	0.7143	− 2.9227
13	40	20	100	200	0.6360	− 3.9306
14	40	40	75	190	0.6565	− 3.6551
15	40	60	50	220	0.6843	− 3.2952
16	40	80	25	210	0.7146	− 2.9183

References

1. Dogaris B, Loya B, Cox J, Philippidis G. Study of landfill leachate as a sustainable source of water and nutrients for algal biofuels and bioproducts using the microalga Picochloromoculatum in a novel scalable bioreactor. BioresourTechnol. 2019;282:18–27.

2. Nithya S, Manigandan S, Gunasekar P, Devipriya J, Saravanan WSR. The effect of engine emission on canola biodiesel blends with TiO2. Int J Ambient Energy. 2018;40(8):838–41.

3. Zhao FX, Shang HY. Role of transportation network on population distribution evolution, Physica A Stat. Mech. Appl. 2021;577

4. Global BP, Worldwide BP. BP Energy Outlook 2030. London;2011

5. Jain IP. Hydrogen the fuel for 21st century. Int J Hydrogen Energy. 2009;34(17):7368–78.

6. Yu MJ. Synthesis of biodiesel from an oil fraction separated from food waste leachate. Korean J Chem Eng. 2011;28(12):2287–92.

7. Khan O, Khan MZ, Khan ME, Goyal A, Bhatt BK, Khan A, Parvez M. Experimental analysis of solar powered disinfection tunnel mist spray system for coronavirus prevention in public and remote places. Mater Today Proc. 2021;46(15):6852–8.

8. Ali N, Farjana I. The effects of air pollution on COVID-19 infection and mortality, a review on recent evidence. Front. Public Health. 2019;8.

9. Travaglio M, Yu Y, Popovic R, Selley L, Leal NS, Martins LM. Links between air pollution and COVID-19 in England. Environ. Pollut. 2021;268(Part A).

10. Cosimo M, Mele M, Schneider N. The relationship between air pollution and COVID-19-related deaths: an application to three French cities. Appl. Energy. 2020;279.

11. Ashman CH, Gao L, Goldfarb JL. Silver nitrate in situ upgrades pyrolysis biofuels from brewer's spent grain via biotemplating. J. Anal Appl. Pyrolysis. 2020;146.

12. El-Shafay AS, Ağbulut U, Attia E, Touileb KL, Gad MS. Waste to energy: production of poultry-based fat biodiesel and experimental assessment of its usability on engine behaviors. Energy. 2023;262(B).

13. Hariram V, Seralathan S, Rajasekaran M, Kumar MD, Padmanabhan S. Effect of metallic nano-additives on combustion performance and emissions of DI CI engine fuelled with palmkernel methyl ester. Int J Veh Struct Syst. 2017;9(2):103–9.

14. Soudagar MEM, Banapurmath NR, Afzal A, Hossain N, Abbas MM, Cader MA, Haniffa M, Naik B, Ahmed W, Nizamuddin S, Mubarak NM. Study of diesel engine characteristics by adding nanosized zinc oxide and diethyl ether additives in Mahua biodiesel–diesel fuel blend. Sci Rep. 2020;10.

15. Panithasan M. Exploring the preparation and usage of low viscous pine oil and rice husk nano additives in a CRDI engine under the effect of water emulsion. SAE Technical Paper;2020

16. Hossain AK, Hussain A. Impact of nanoadditives on the performance and combustion characteristics of neat jatropha biodiesel. Energies. 2019;12(5).

17. Yaqoob H, Teoh YH, Sher F, Farooq MU, Jamil MA, Kausar Z, Sabah NU, Shah MF, Rehman HZU, Rehman AU. Potential of waste cooking oil biodiesel as renewable fuel in combustion engines: a review. Energies. 2021;14(9).

18. Yadav AK, Khan O, Khan ME. Utilization of high FFA landfill waste (leachates) as a feedstock for sustainable biodiesel production: its characterization and engine performance evaluation. Environ Sci Pollut Res. 2018;25:32312–20.

19. Venu H, Venkataraman D, Purushothaman P, Vallapudi DR. Eichhornia crassipes biodiesel as a renewable green fuel for diesel engine applications: performance, combustion, and emission characteristics. Environ Sci Pollut Res. 2019;26:18084–97.

20. Kulkarni MG, Dalai AK. Waste cooking oil- an economical source for biodiesel a review. Ind Eng Chem Res. 2006;45(9):2901–13.

21. Nutakki PK, Gugulothu SK, Ramachander J, Sivasurya M. Effect Of n-amyl alcohol/biodiesel blended nano additives on the performance, combustion and emission characteristics of CRDi diesel engine. Environ Sci Pollut Res. 2022;29:82–97.

22. Karthikeyan S, Prathima A. Emission analysis of the effect of doped nano-additives on biofuel in a diesel engine. Energy Sources A Recovery Utilization Environ Effects. 2016;38(24):3702–8.

23. Orsa I, Sarıkoçb S, Atabani AE, Ünalan S, Akansu SO. The effects on performance, combustion and emission characteristics of DICI engine fuelled with TiO2 nanoparticles addition in diesel/biodiesel/n butanol blends. Fuel. 2018;234:177–88.

24. Hosseini SS, Najafi G, Ghobadian B, Mamat R, Ebadi MT, Yusaf T. Novel environmentally friendly fuel: the effects of nanographene oxide additives on the performance and emission characteristics of diesel engines fuelled with Ailanthus altissima biodiesel. Renew Energy. 2018;125:104–10.

25. Hossain N, Mahlia TMI, Saidur R. Latest development in microalgae-biofuel production with nano-additives. Biotechnol Biofuels. 2019;12.

26. Gao L, Goldfarb JL. Solid waste to biofuels and heterogeneous sorbents via pyrolysis of wheat straw in the presence of fly ash as an in situ catalyst. J Anal Appl Pyrol. 2019;137:96–105. https://doi.org/10.1016/j.jaap.2018.11.014.

27. Raheman H, Jena PC, Jadav SS. Performance of a diesel engine with blends of biodiesel (from a mixture of oils) and high-speed diesel. Int J Energy Environ Eng. 2013;4

28. Arguelles EDLR, Laurena AC, Monsalud RG, Martinez-Goss MR. Fatty acid profile and fuel-derived physico-chemical properties of biodiesel obtained from an indigenous green microalga, Desmodesmus sp. (I-AU1), as potential source of renewable lipid and high quality biodiesel. J ApplPhycol. 2018;30:411–9.

29. Gad MS, Kamel BM, Badruddin IA. Improving the diesel engine performance, emissions and combustion characteristics using biodiesel with carbon nanomaterials. Fuel. 2021;288.

30. Kodate SV, Yadav AK, Kumar GN. Combustion, performance and emissionanalysis of preheated KOME biodiesel as an alternate fuel for a diesel engine. J Therm Anal Calorim. 2020;141:2335–45.

31. Rezania S, Mahdinia S, Oryani B, Cho J, Kwon EE, Bozorgian A, Nodeh HR, Darajeh N, Mehranzamir K. Biodiesel production from wild mustard (Sinapis-Arvensis) seed oil using a novel heterogeneous catalyst of LaTiO3 nanoparticles, Fuel. 2022;307

32. Saraee SH, Jafarmadar S, Taghavifar H, Ashrafi SJ. Reduction of emissions and fuel consumption in a compression ignition engine using nanoparticles. Int J Environ Sci Technol. 2015;12:2245–52.

33. Lakshmi VR, Jaikumar S, Srinivas V. A comprehensive review on the effect of nanoparticle dispersed diesel-biodiesel blends fuelled CI engine. J Inst Eng India Ser C. 2021;102:495–505.

34. Devarajan Y, Nagappan B, Subbiah G. A comprehensive study on emission and performance characteristics of a diesel engine fueled with nanoparticle-blended biodiesel. Environ Sci Pollut Res. 2019;26:10662–72.

35. Khan O, Khan MZ, Ahmad N, Qamer A, Alam MT, Siddiqui AH. Performance and emission analysis on palm oil derived biodiesel coupled with aluminium oxide nanoparticles. Mater. Today Proc. 2019;46.

36. Jones M, Li CH, Afjeh A, Peterson GP. Experimental study of combustion characteristics of nanoscale metal and metal oxide additives in biofuel (ethanol). Nanoscale Res Lett. 2011;6:246.

37. Krishnasamy AA, Bukkarapu KA. A comprehensive review of biodiesel property prediction models for combustion modeling studies. Fuel. 2021;302.

38. Sharma PK, Sharma D, Soni SL, Jhalani A. Characterization of the non-road modified diesel engine using a novel Entropy-VIKOR approach: experimental investigation and numerical simulation. J. Energy Resour. Technol. ASME. 2019;141(8).

39. Sivaraja CM, Sakthivel G. Compression ignition engine performance modelling using hybrid MCDM techniques for the selection of optimum fish oil biodiesel blend at different injection timings. Energy. 2017; 139(15).

40. Debbarma B, Chakraborti P, Bose PK, Deb M, Banerjee R. Exploration of PROMETHEE II and VIKOR methodology in a MCDM approach for ascertaining the optimal performance-emission trade-off vantage in a hydrogen-biohol dual fuel endeavour. Fuel. 2017;210:922–35.

41. Zavadskas EK, Čereška A, Matijošius J, Rimkus A, Bausys R. Internal combustion engine analysis of energy ecological parameters by neutrosophic MULTIMOORA and SWARA methods. Energies. 2019;12(8).

42. Vellaiyan S, Koduvayur SN. MROof diesel engine operating parameters running with water-in-diesel emulsion fuel. Therm Sci. 2017;21:427–39.

43. Karnwal A, Hasan MM, Kumar N, Siddiquee AN, Khan ZA. MROOf diesel engine performance parameters using thumba biodiesel-diesel blends by applying the taguchi method and grey relational analysis. Int J Autom Technol. 2011;12(4):599–610.

44. Erdoğan S, Aydın S, Balki MK, Sayin C. Operational evaluation of thermal barrier coated diesel engine fueled with biodiesel/diesel blend by using MCDM method base on engine performance, emission and combustion characteristics. Renew Energy. 2019;151:698–706.

45. Lamas MI, Castro-Santos L, Rodriguez CG. Optimization of a multiple injection system in a marine diesel engine through a multiple-criteria decision-making approach. J Mar Sci Eng. 2020;8(11).

46. Soudagar MEM, Nik-Ghazali NN, Kalam MA, Badruddin IA, Banapurmath N, Khan TY, et al. The effects of graphene oxide nanoparticle additive stably dispersed in dairy scum oil biodiesel-diesel fuel blend on CI engine: performance, emission and combustion characteristics. Fuel. 2019;257:116015.

47. Soudagar MEM, Nik-Ghazali NN, Kalam MA, Badruddin IA, Banapurmath NR, Ali MAB, et al. An investigation on the influence of aluminium oxide nano-additive and honge oil methyl ester on engine performance, combustion and emission characteristics. Renewable Energy. 2020;146:2291–307.

48. Soudagar MEM, Mujtaba MA, Safaei MR, Afzal A, Ahmed W, Banapurmath NR, Taqui SN. Effect of Sr@ ZnO nanoparticles and Ricinus communis biodiesel-diesel fuel blends on modified CRDI diesel engine characteristics. Energy. 2021;215:119094.

49. Khan H, Soudagar MEM, Kumar RH, Safaei MR, Farooq M, Khidmatgar A, et al. Effect of nano-graphene oxide and n-butanol fuel additives blended with diesel—Nigella sativa biodiesel fuel emulsion on diesel engine characteristics. Symmetry. 2020;12(6):961.

50. Mujtaba MA, Kalam MA, Masjuki HH, Gul M, Soudagar MEM, Ong HC, Yusoff M. Comparative study of nanoparticles and alcoholic fuel additives-biodiesel-diesel blend for performance and emission improvements. Fuel. 2020;279: 118434.

51. Khan O, Khan MZ, Bhatt BK, Alam MT, Tripathi M. Multi-objective optimization of diesel engine performance, vibration and emission parameters employing blends of biodiesel, hydrogen and cerium oxide nanoparticles with the aid of response surface methodology approach. Int J Hydrogen Energy. 2023;48(56):21513–29.

52. Phadke M. Quality engineering using robust design. 1989;31–50.

53. Elsheikh AH, Sharshir SW, Kabeel AE, Sathyamurthy R. Application of Taguchi method to determine the optimal water depth and glass cooling rate in solar stills. Scientia-Iranica. 2021;28(2):731–42.

54. Jeyapaul R, Shahabudeen P, Krishnaiah K. Quality management research by considering multi-response problems in the Taguchi method—a review. Int J Adv ManufT echnol. 2005;26(11):1331–7.

55. Mehat NM, Kamaruddin S. Quality control and design optimisation of plastic product using Taguchi method: a comprehensive review. Int J Plast Technol. 2012;16(2):194–209.

56. Singaravel B, Selvaraj T. Application of Taguchi method for optimization of parameters in turning operation. J Manuf Sci Prod. 2016;16(3):183–7.

57. Lance AE. Quality by design Taguchi methods and US industry;1994.

58. Khan O, Yadav AK, Khan ME, Parvez M. Characterization of bioethanol obtained from Eichhornia Crassipesplant; its emission and performance analysis on CI engine. Energy Sources A Recovery Utilization Environ Effects. 2019;43:1–11.

59. Keshavarz-Ghorabaee M, Amiri M, Zavadskas EK, Turskis Z, Antucheviciene J. Determination of objective weights using a new method based on the removal effects of criteria (MEREC). Symmetry. 2021;13(4).

60. Stević Ž, Pamučar D, Puška A, Chatterjee P (2020) Sustainable supplier selection in healthcare industries using a new MCDM method: measurement of alternatives and ranking according to compromise solution (MARCOS). Comput Ind Eng 140.

61. Mohanty A, Nag KS, Bagal DK, Barua A, Jeet S, Mahapatra SS, Cherkia H. Parametric optimization of parameters affecting dimension precision of FDM printed part using hybrid Taguchi-MARCOS-nature inspired heuristic optimization technique. Mater Today Proc. 2022;50(5):893–903.

62. Stević Ž, Brković N. A novel integrated FUCOM-MARCOS model for evaluation of human resources in a transport company. Logistics. 2020;4(1).

63. Puška A, Stojanović I, Maksimović A, Osmanović N. Evaluation software of project management used measurement of alternatives and ranking according to compromise solution (MARCOS) method. Oper Res Eng Sci Theory Appl. 2020;3(1).

64. Stanković M, Stević Ž, Das DK, Subotić M, Pamučar D. A new fuzzy MARCOS method for road traffic risk analysis. Mathematics. 2020;8(3)

65. Naddaf A, Heris SZ. Experimental study on thermal conductivity and electrical conductivity of diesel oil-based nanofluids of graphene nanoplatelets and carbon nanotubes. IntCommun Heat Mass Transfer. 2018;1(95):116–22.

66. Selvan VAM, Anand R, Udayakumar M. Effect of cerium oxide nanoparticles and carbon nanotubes as fuel-borne additives in diesterol blends on the performance, combustion and emission characteristics of a variable compression ratio engine. Fuel. 2014;130:160–7.

67. Yaşar A, Keskin A, Yıldızhan Ş, Uludamar E. Emission and vibration analysis of diesel engine fuelled diesel fuel containing metallic based nanoparticles. Fuel. 2019;1(239):1224–30.

68. Keskin A, Yaşar A, Yıldızhan Ş, Uludamar E, Emen FM, Külcü N. Evaluation of diesel fuel-biodiesel blends with palladium and acetylferrocene-based additives in a diesel engine. Fuel. 2018;15(216):349–55.

69. Bharathiraja R, Amirthagadeswaran KS, Praveenkumar N, Periyasamy DS, Babu KR. Study on characteristics of CI engine using nano additive blended diesel fuel. Int J ApplEng Res. 2015;10(67):328–34.

70. Shaafi T, Velraj R. Influence of alumina nanoparticles, ethanol and isopropanol blend as additive with diesel–soybean biodiesel blend fuel: Combustion, engine performance and emissions. Renew Energy. 2015;1(80):655–63.

71. Khulief S, Aboul-Fotouh TM. Experimental investigation of upgraded diesel fuel with copper oxide nanoparticles on performance and emissions characteristics of diesel engine. J Energy Power Eng. 2017;11:541–52.

72. El-Seesy AI, Attia AM, El-Batsh HM. The effect of Aluminium oxide nanoparticles addition with Jojoba methyl ester-diesel fuel blend on a diesel engine performance, combustion and emission characteristics. Fuel. 2018;15(224):147–66.

73. Aalam CS, Saravanan CG, Kannan M. Experimental investigations on a CRDI system assisted diesel engine fuelled with aluminium oxide nanoparticles blended biodiesel. Alexandria Eng J. 2015;54(3):351–8.

74. Soukht HS, Jafarmadar S, Alizadeh-Haghighi E, Ashrafi SJ. Experimental investigation of pollution and fuel consumption on a CI engine operated on alumina nanoparticles—diesel fuel with the aid of artificial neural network. Environ Prog Sustain Energy. 2016;35(2):540–6.

75. Krupakaran RL, Hariprasasd T, Gopalakrishna A, Babu P. The performance and exhaust emissions investigation of a diesel engine using γ-Al2O3 nanoparticle additives to biodiesel. Carbon Manag. 2016;7(3):233–41.

76. Channappagoudra M. Effect of copper oxide nanoadditive on diesel engine performance operated with dairy scum biodiesel. Int J Ambient Energy. 2018;42(5):1–10.

77. Chen YS, Yang CM, Hoang TTN, Tsai DH. Porous magnesia-alumina composite nanoparticle for biodiesel production. Fuel. 2021;285.

78. Alhikami AF, Chia-En Y, Wei-Cheng W. A study of the spray ignition characteristics of hydro-processed renewable diesel, petroleum diesel, and biodiesel using a constant volume combustion chamber. Combust Flame. 2021;223:55–64.

79. Lakshmi RV, Jaikumar S, Srinivas V, Rajasekhar M. Vibration and noise study on the direct injection compression ignition engine running with nanoparticle dispersed abrusprecatorius biodiesel blend. Silicon. 2021;